ROMANIAN JOURNAL OF INFORMATION SCIENCE AND TECHNOLOGY
Volume **27**, Number 2, 2024, 196–206

Accurate Numerical Methods for Modeling Forward Characteristics of High Temperature Capable Schottky Diodes

Gheorghe PRISTAVU[1], Dan-Theodor ONEAȚĂ[1], Răzvan PASCU[1,2,*], Alina Elena MARCU[1], Matei-Constantin ȘERBĂNESCU[1], Andrei ENACHE[1], Florin DRĂGHICI[1], and Gheorghe BREZEANU[1]

[1]National University of Science and Technology POLITEHNICA Bucharest, Bucharest, Romania
[2]National Institute for R&D in Microtechnology - IMT Bucharest, Bucharest, Romania
E-mail: razvan.pascu@imt.ro[*]

Abstract. The paper discusses two algorithms for accurately determining solutions to the transcendental thermionic emission equation, which is the cornerstone of forward electrical behavior in Schottky diodes. The numerical techniques are developed based on the Newton-Raphson and Halley methods. Both approaches use distinct forms for the thermionic emission expression, emphasizing robustness against numerical overflows. Parameter initialization, complexity and applicability are discussed for each technique. A comparison is carried out between forward characteristics simulated with the two methods, which are then also used for characterizing real SiC-Schottky diodes. Results evince complete compatibility and highly accurate approximations of experimental measurements ($R^2 \cong 99.9\%$) on devices with different contact compositions.

Key-words: Forward characteristics; numerical methods; Schottky diode; thermionic emission equation.

1. Introduction

High quality metal-semiconductor interfaces represent the primary indicator of a technological process's level of maturity [1]. Indeed, ohmic contacts [2] are present universally in any finished electronic device, while Schottky contacts [3] with stable and predictable electrical behavior indicate that a technology is well on its way to becoming mainstream. Such was the case for silicon carbide (SiC) device processing, where the Schottky diode was the first commercially available device, followed closely by MOS transistors. Presently, SiC technology is proliferating in power applications [4], with intense scientific efforts being channeled towards high-performing sensors [5].

Despite being a pivotal structure for many decades, the Schottky diode, governed by the thermionic emission (TE) current conduction mechanism, is still challenging to properly characterize [1], [4], [5]. As these devices have considerably expanded their operational temperature ranges [6], puzzling effects, such as contact inhomogeneity [6]-[12] have emerged with dominating impact on electrical behavior. Unexpectedly, contemporary approaches continue to rely on traditional techniques or have only recently transitioned to seamless computer-aided modeling [13], [14] as opposed to concentrating on developing and adapting models to account for these spurious occurrences.

The prediction of electronic device behavior has begun to be achievable with the emergence of neural network-powered optimization methods [15], through the use of arbitrary functions rather than relying on the physical significance of the employed parameters. Methods such as artificial neural network, advanced swarm intelligence, equilibrium optimizer [16], and artificial bee colony are employed to determine the electrical parameters of Schottky diodes. Using a swarm intelligence technique known as the dragonfly algorithm (DA), in [17], the impact of temperature on these parameters was examined. In [18], the authors determined them using a variety of meta-heuristic optimization algorithms, including equilibrium optimizer (EO), artificial hummingbirds algorithm (AHA), genetic algorithm (GA), Dragonfly Algorithm (DA), ant lion algorithm (ALO), and particle swarm optimization (PSO). The outcomes demonstrated that the estimation performance of the artificial hummingbirds algorithm (AHA) was superior to that of the alternative methods employed. It was determined that artificial intelligence data can be used to compute electrical parameters. In [19], the authors modeled the temperature-dependent current-voltage characteristics of Schottky diodes by employing a number of widely used machine learning techniques. Rabehi et al. [16] used the equilibrium optimizer algorithm to determine diode parameters, which were in good agreement with those extracted by conventional means. Çolak et al. [20] used artificial neural networks (ANNs) to simulate temperature-dependent current-voltage characteristics, with successful results. In [21], a neural network model was developed to predict electrical parameters with an average deviation of 0.11%.

While the aforementioned approaches prove that emerging computing techniques have the potential to lead the development of the Schottky diode characterization field, they are still at very early stages. Most of the solutions only focus on actual forward curve fitting, without particular focus (or reliance) on the physical relevance of obtained parameters. A bridging between these approaches and consecrated advanced analytical modeling of the Schottky contact is necessary in order to ensure the comprehensive utility of results (for performance assessment, technology improvement and application-simulations).

Acknowledging the potential justification and advantages of these current methodologies, this paper investigates high-fidelity simulation methods for the TE-based conduction mechanism of a Schottky diode over ample temperature ranges. Section 2 discusses the context and cur-

rent issues in solving the thermionic emission equation. In order to ensure accurate modeling of actual device behavior, two prospective algorithms are analyzed and compared in Section 3, with respect to their convergence speed and implementation complexities. The simulated and experimental results given in Section 4 constitute a key step towards implementation of an accurate, automated characterization tool, driven by emerging optimization algorithms. Finally, conclusions are drawn in Section 5.

2. Context and Issues

As previously stated, a Schottky diode's forward current (I_F) as a function of applied voltage (V_F) is described by the TE equation:

$$I_F = I_S \left[\exp\left(\frac{V_F - I_F R_S}{n V_{th}} \right) - 1 \right], \tag{1}$$

where

$$I_S = A_S A_n T^2 \exp\left(-\frac{\Phi_{Bn}}{V_{th}} \right), \tag{2}$$

A_S is the nominal contact area, A_n is the Richardson constant, T is ambient temperature, V_{th} is its associated thermal voltage, Φ_{Bn} is the Schottky barrier height (SBH), R_S is the series resistance and n is the ideality factor. Equation (1) is predominantly used in applications pertaining to Schottky diode characterization, either directly or as the underlying model (with different functions associated to its key parameters).

Usual simplifications of (1) include neglecting the "-1" end term (which is only impactful at very low bias, where V_F is comparable to $3V_{th}$) or not considering the series resistance effect (significant at higher voltages, where the device essentially exhibits ohmic behavior). Under such assumptions, the natural logarithm of (1) becomes a linear dependence between $\ln(I_F)$ and V_F. The interpretation of slope and intercept values for this function, at different temperatures, has been the cornerstone of Schottky diode parameter extraction for decades. However, with the rapid technological advances in the field of wide bandgap semiconductor devices, fore fronted by Schottky diodes, it quickly became obvious that this technique produces misleading or outright erroneous results when applied over wide temperature ranges. The obvious reason is that both V_{th} and I_S increase substantially with temperature, which narrow down or completely eliminate the bias interval where the aforementioned simplifications are valid. Perhaps an even more impactful cause is the presence of *inhomogeneity* on the contact surface, which determines a real Schottky diode to behave as multiple such devices connected in parallel [6]-[12]. These parasitic-diodes can considerably influence current flow, especially at low temperatures. Since their main parameter values are uncontrollable, especially R_S, finding a bias interval where all of these devices may be modeled by a simplified TE equation becomes nearly impossible.

Because of these considerations, it is clear that modern modeling of a Schottky diode requires methods to accurately estimate solutions for the complete TE eq. (1), over an extensive range of parameter values. However, it can be observed in (1) that $I_F(V_F)$ is a transcendental function, which is not tractable analytically. A potential work-around may be switching to a $V_F(I_F)$ representation, which can be completely solved with conventional methods. However, this approach is almost never used, mainly due to the following taxonomy: (a) data acquisition is preferentially performed as a function of applied voltage (e.g. I-V, C-V measurements) and (b) modeling

and optimization is usually evaluated per individual data point. Furthermore, some parameters in (1) explicitly relate to V_F dependence (e.g. voltage dependence of SBH is expressed by the introduction of *n*, while keeping Φ_{Bn} constant). Other approaches, such as using the Lambert W function [22] can offer analytically-solvable versions of (1). However the Lambert W itself cannot be exactly determined. As such, iterative algorithms become an attractive alternative in order to accurately estimate I_F at each given V_F, usually for fixed forward voltage steps.

3. Techniques to Simulate Schottky Diode $\mathbf{I_F}$ $\mathbf{(V_F)}$ Dependence

Two methods of iteratively solving (1) are investigated. For each, the TE equation is expressed in a convenient form, ensuring robustness to numerical overflows.

3.1. The Newton-Raphson technique

One of the consecrated methods of estimating the solution of an equation, which isn't analytically tractable, is the Newton-Raphson technique (NRT). Given a differentiable function $f(x)$, if you estimate its root as x_0, then a more accurate value would be:

$$x_1 = x_0 - \frac{f(x_0)}{f'(x_0)}, \tag{3}$$

where f' is the first order derivative of the function. This process can be continued until the estimate is considered sufficiently precise.

In order to implement this approach for estimating $I_F(V_F)$, equation (1) is rewritten as:

$$\ln\left(\frac{I_F + I_S}{I_S}\right) = \frac{V_F - I_F R_S}{nV_{th}}. \tag{4}$$

Since the value of I_S can span tens of orders of magnitude for different SBH over wide temperature ranges, (4) was further reformulated

$$nV_{th}\ln\left(\frac{I_F + I_S}{A_S A_n T^2}\right) + n\Phi_{Bn} = V_F - I_F R_S, \tag{5}$$

giving a final form of the function to be processed by the Newton-Raphson technique, f [14]:

$$f(I_{F,0}) = nV_{th}\ln\left(\frac{I_{F,0} + I_S}{A_S A_n T^2}\right) - V_F + n\Phi_{Bn} + I_{F,0}R_S. \tag{6}$$

Thus, we can determine the approximation of the forward current as:

$$I_{F,n+1} = I_{F,n} - \frac{nV_{th}\ln\left(\frac{I_{F,n}+I_S}{A_S A_n T^2}\right) - V_F + n\Phi_{Bn} + I_{F,n}R_S}{\frac{nV_{th}}{I_{F,n}+I_S} + R_S}. \tag{7}$$

Expression (7) has the advantage that all of its terms are robust against overflows. To further ensure this aspect, in the practically implemented version of the algorithm, we capped the minimum exponent for I_S calculations. A value of (-70) was selected, far exceeding the precision of conventional practical measurement systems. Since (7) sums this parameter with $I_{F,n}$ at every occurrence, the overall method accuracy is virtually unaffected. The stopping points of the

algorithm were set when either two subsequent estimations reached a ratio higher than 0.9999 or one thousand iterations are performed.

A critical element for proper convergence of the NRT approach is selecting an adequate initial estimation ($I_{F,0}$). For our implementation, two cases are considered. For low bias, where series resistance has negligible impact on forward characteristics,

$$I_{F,0} \cong A_S A_n T^2 \exp\left(\frac{V_F - n\Phi_{Bn}}{nV_{th}}\right) \tag{8}$$

ensures proper current estimation and overflow robustness until the series resistance effect becomes predominant. Here, at higher bias, when condition (8) leads to final current ($I_{F,n}$) many times lower than $I_{F,0}$, a new definition for the initial estimate is employed, ensuring that it stays close to the actual solution [14]:

$$I_{F,0} = I_{F,n(p)} + \frac{\Delta V_F}{R_S}, \tag{9}$$

where $I_{F,n(p)}$ is the estimated value for the previous data point and ΔV_F is the measurement voltage step.

3.2. Halley's method

One notable drawback of the previous technique is that the accurate initial estimates require sequential determination of currents, which is unsuitable for modern parallel computing approaches. Additionally, the convergence speed is just quadratic. As such, a better performing approximation may be obtained using Halley's method (HM). According to it, the estimation of a function's root is subsequently improved as such:

$$x_{n+1} = x_n - \frac{2g(x_n)g'(x_n)}{2g'(x_n)^2 - g(x_n)g''(x_n)}, \tag{10}$$

where g'' is the second order derivative of the function.

In this case, the expression of the $g(x)$ function is sought to be

$$g(x) = x + e^x - a. \tag{11}$$

In order to achieve this form, (1) was rewritten as

$$I_F - I_S \exp\left(\frac{V_F - I_F R_S}{nV_{th}}\right) = -I_S. \tag{12}$$

After multiplying by $-R_S$, adding V_F and dividing by nV_{th}, we obtain

$$\frac{V_F - I_F R_S}{nV_{th}} + \frac{I_S R_S}{nV_{th}} \exp\left(\frac{V_F - I_F R_S}{nV_{th}}\right) = \frac{V_F + I_S R_S}{nV_{th}}. \tag{13}$$

We add $\ln \frac{I_S R_S}{nV_{th}}$ and move the factor $\frac{I_S R_S}{nV_{th}}$ to the exponent, yielding

$$\begin{aligned} \ln\left(\frac{I_S R_S}{nV_{th}}\right) + \frac{V_F - I_S R_S}{nV_{th}} + \exp\left[\ln\left(\frac{I_S R_S}{nV_{th}}\right) + \frac{V_F - I_F R_S}{nV_{th}}\right] = \\ = \ln\left(\frac{I_S R_S}{nV_{th}}\right) + \frac{V_F + I_S R_S}{nV_{th}}. \end{aligned} \tag{14}$$

Finally, the desired expression (11) can be achieved by denoting

$$a = \ln\left(\frac{I_S R_S}{nV_{th}}\right) + \frac{V_F + I_S R_S}{nV_{th}}, \tag{15}$$

$$x = \ln\left(\frac{I_S R_S}{nV_{th}}\right) + \frac{V_F - I_F R_S}{nV_{th}}. \tag{16}$$

The value of x, given by (16), is optimized using (10) and (11), yielding

$$x_{n+1} = x_n - \frac{2(x_n + e^{x_n} - a)(1 + e^{x_n})}{2(1 + e^{x_n})^2 - (x_n + e^{x_n} - a)e^{x_n}}. \tag{17}$$

To avoid overflows and improve numerical stability, for a values higher than zero, equation (7) was normalized by e^{-x_n} (both nominator and denominator were divided by this value). Finally, according to the procedure described in [22], we initialize the optimization algorithm as:

$$x_0 = \begin{cases} a, & a < 1/e \\ \ln(a), & a \geq 1/e \end{cases} \tag{18}$$

After the x estimate is obtained using Halley's method, the forward current can be determined from (15) [14]:

$$I_F = \frac{1}{R_S}\left[V_F - nV_{th}\left(x - \ln\frac{I_S R_S}{nV_{th}}\right)\right]. \tag{19}$$

This approach has cubic convergence speed and allows simultaneous estimation of I_F values, at all forward voltages and temperatures. Its drawback is that it requires second order derivative calculations, which can be difficult to even estimate automatically. In our case however, the suitable definition (11) allows easy calculation of (17) and its normalized variant.

4. Results

The I_F-V_F simulation methods presented in Section 3 were practically implemented in separate programming languages. C++ was used for the Newton-Raphson technique, while Python was preferred for Halley's approximation, due to its suitability in parallel computing. Figure 1 presents simulated forward characteristics for a 1 mm^2 SiC-Schottky contact area, using both approaches, over the $25 - 400$°C temperature range. High $(1.7V)$ and low $(1.2V)$ values for the Schottky barrier were considered, corresponding to specific high-temperature and efficient switching applications, respectively. A series resistance $R_S = 10\Omega$ was used. Notably, we enforced the ideality factor limit of $n = 1.03$ throughout the temperature and bias range, as this is the highest value corresponding image-force lowering in pure, TE-based conduction [8]. Excellent agreement between both simulation techniques is noted, with coefficients of determination (R^2) above 99.99% [14].

The adequacy of the two methods for simulating the behavior of practical devices was also assessed. Forward curves of Schottky diodes with various contacts were measured in encompassing temperature domains. High barrier Ni/4H-SiC and low SBH Ti/4H-SiC and Cr/4H-SiC contacts were selected for analysis.

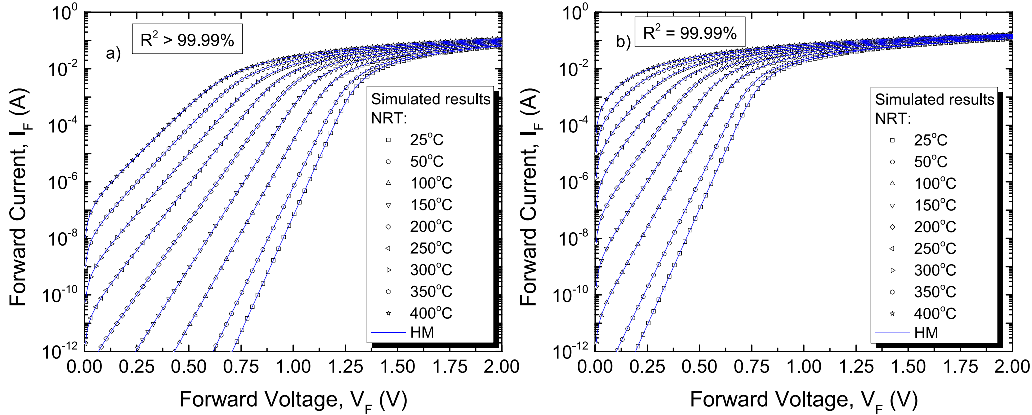

Fig. 1. Simulated forward characteristics for a 1 mm^2 SiC-Schottky contact area, using NRT (symbols) and HM (lines), over $25 - 400°C$: a) High SBH; b) Low SBH [14].

Figure 2 depicts the measurement-simulation comparison, carried out both at room and at suitably high temperatures ($400°C$ for Ni-SiC and $227°C$ for Ti-SiC). Simulation parameters are given in Table 1. In order to partially account for contact inhomogeneity, the effective area (A_{eff}) was considered instead of A_S [10]. Table 1 values confirm the practical relevance of the simulation parameters considered in the initial NRT-HM comparison (Figure 1).

Table 1. Ti/4H-SiC and Ni/4H-SiC Simulation Parameters [14]

Schottky contact	Parameters			
	Φ_{Bn} [V]	A_{eff} [mm^2]	n	R_S [Ω]
Ti/4H-SiC	1.22	0.82	1.03	$7 - 9.5$
Ni/4H-SiC	1.7	0.03		$2.5 - 8$

In Figure 2, both simulated curves are in very good agreement ($R^2 > 99.99\%$) [14]. They closely approximate measurements, even at high temperature and very low bias levels, as confirmed by the high value for R^2 given in Figure 2 inset. Notably, the transition regions between exponential and linear I_F-V_F dependence (corresponding to R_S effects overtaking thermionic emission) are also well reflected by simulations.

Finally, the NRT and HM were used to simulate forward behavior of a Cr/4H-SiC Schottky diode over an extensive temperature span ($22°C - 406°C$), depicted in Figure 3, with parameters given in Table 2. It can be seen that, for such a low SBH contact, the forward characteristics exhibit clear exponential current-voltage behavior only up to $227°C$, similar to the Ti/4H-SiC device in Figure 2. Above this limit, the considerable increase in thermal voltage and series resistance make all the terms in the thermionic emission equation significant. Furthermore, clear evidence of contact inhomogeneity can be observed for the $406°C$ temperature level (red colored curve in Figure 3, with a significantly different allure). At this overstretching point, the series resistance of the contact region that was dominantly responsible for current flow surges dramatically. In this case, the *p-diode* inhomogeneity model, with two parallel-diodes, is suitable [10]. Their parameters are also given in Table 2. As bias increases, the high R_S suppresses the Dp1 contribution to total I_F. This enables Dp2, with a previously negligible effect, albeit with a much higher effective area, to overtake conduction.

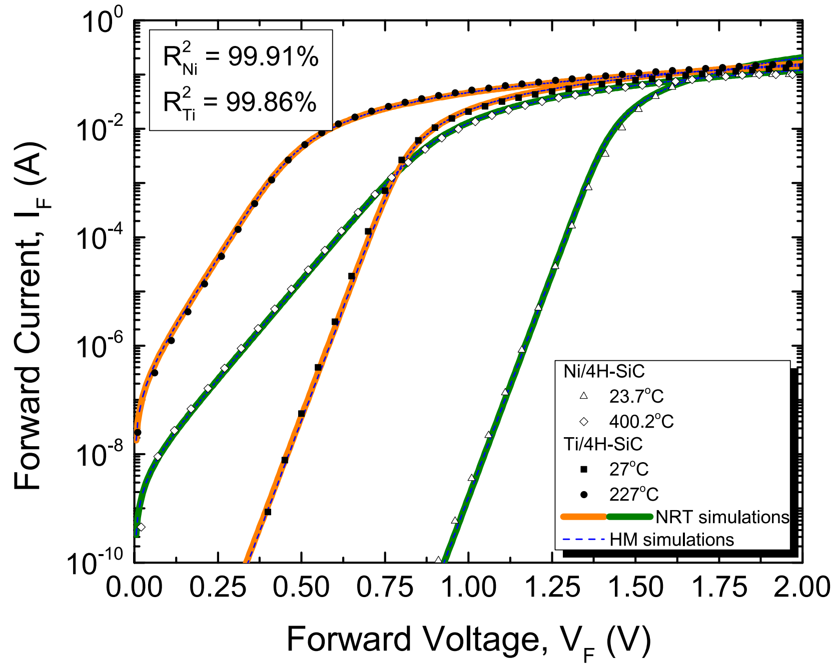

Fig. 2. Measured forward curves (symbols) for Schottky diodes with Ni/4H-SiC and Ti/4H-SiC contacts, together with NRT (lines) and HM (dashed lines) simulated data [14].

Despite this situation, both simulation methods produce highly accurate fittings of measured data, once again with R^2 around 99.9%, even above $227°C$. More so, the forward characteristic at $406°C$ is excellently replicated, when considering the lumped contributions of the two aforementioned parallel-diodes (Dp1, Dp2 - Table 2).

The results presented in this section confirm the suitability of the two methods in simulating the forward behavior of practical Schottky diodes over exhaustive temperature intervals. Furthermore, highly promising prospects of integration in automated inhomogeneity modeling tools are evinced.

Even though both the NRT and HM produce nearly identical results, for the parameter extraction and optimization processes, which entail a large complexity order, Halley's method is preferred. This is due to its compatibility with parallel computing. The validity of obtained parameters can be confirmed with the NRT, which boast accurate and robust simulation capabilities over any complete set of realistic temperature and bias regions.

Table 2. Cr/4H-SiC Simulation Parameters

Cr/4H-SiC		**Parameters**			
		Φ_{Bn} $[V]$	A_{eff} $[mm^2]$	n	R_S $[\Omega]$
$22°C - 386°C$		0.9	$3.29 \cdot 10^{-3}$	1.03	$22 - 59$
$406°C$	Dp1	0.9	$3.29 \cdot 10^{-3}$		420
	Dp2	1.7	0.126		60

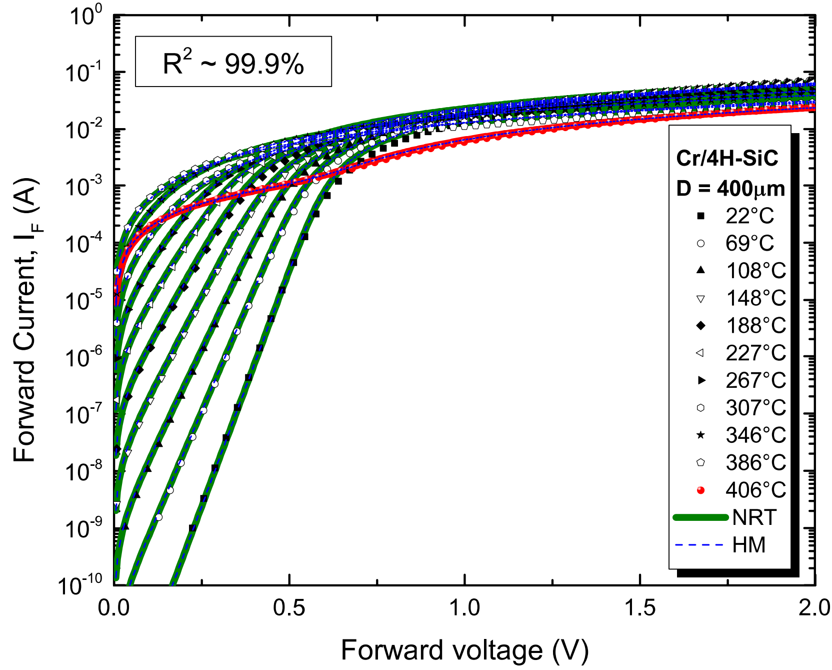

Fig. 3. Measured forward curves (symbols) for a Schottky diode with Cr/4H-SiC contact, together with NRT (lines) and HM (dashed lines) simulated data.

5. Conclusions

In this paper, two numerical optimization methods for solving the thermionic emission equation, which predominantly models Schottky diode forward electrical behavior, were analyzed, implemented and compared. Both approaches relied on custom reformulations of the TE expression in order to achieve a form which is robust against numerical overflows. The first method uses the Newton-Raphson algorithm to quickly converge towards an accurate solution with a minimal amount of iterations. This is achieved by reusing previous solutions as initialization for subsequent data points. The second approach utilizes Halley's method, which incorporates second-order-derivative information, to reach even faster convergence speed which is further enhanced by its parallel-computing compatibility. Thus, this technique enables the computation of all estimates at the same time.

Both methodologies offer almost identical estimations ($R^2 \cong 99.99\%$) between them, which validates the relevance of simulations. Experimental measurements of practical SiC-Schottky diodes were carried out over encompassing temperature intervals. Samples with Ni, Ti and Cr Schottky metals were characterized, in order to account for a relevant spread of barrier heights. The extracted parameters were used to simulate forward characteristics using the aforementioned numerical techniques. An excellent replication of experimental behavior was obtained with both methods ($R^2 \cong 99.9\%$) over the entire temperature range (room - $400°$C). Notably, these performances held up even when characterizing a low-barrier device (with Cr/4H-SiC contact) much above its normal operating temperatures.

Thus, the NRT and HM can be integrated into advanced inhomogeneity models, offering

accurate simulation capabilities and setting the groundwork for developing automated characterization tools.

Acknowledgements. This work was supported by grants of the Ministry of Research, Innovation and Digitization, CCCDI - UEFISCDI, project numbers PN-III-P2-2.1-PED-2021-2688 and PN-III- P1-1.1-TE-2021-0231, within PNCDI III, and by a grant from the National Program for Research of the National Association of Technical Universities - GNAC ARUT 2023, contract no. 37/9.10.2023.

References

[1] F. ROCCAFORTE, M. VIVONA, G. GRECO, R. LO NIGRO, F. GIANNAZZO, S. RASCUNÀ and M. SAGGIO, *Metal/semiconductor contacts to silicon carbide: Physics and technology*, Materials Science Forum **924**, 2018, pp. 339–344.

[2] M. SPERA, G. GRECO, R. Lo NIGRO, C. BONGIORNO, F. GIANNAZZO, M. ZIELINSKI, F. LA VIA and F. ROCCAFORTE, *Ohmic contacts on n-type and p-type cubic silicon carbide (3C-SiC) grown on silicon*, Materials Science in Semiconductor Processing **93**, 2019, pp. 295–298.

[3] P. GODIGNON, X. JORDA, M. VELLVEHI, X. PERPINA, V. BANU, D. LOPEZ, J. BARBERO, P. BROSSELARD and S. MASSETTI, *SiC Schottky diodes for harsh environment space applications*, IEEE Transactions on Industrial Electronics **58**(7), 2011, pp. 2582–2590.

[4] T. KIMOTO and H. WATANABE, *Defect engineering in SiC technology for high-voltage power devices*, Applied Physics Express **13**(12), 2020, paper 120101.

[5] V. MOISE, F. DRAGHICI, G. PRISTAVU, R. PASCU, D. T. ONEATA and G. BREZEANU, *Intelligent Temperature Sensor with SiC Schottky Diode*, Proceedings of 2022 International Semiconductor Conference, Poiana Brasov, Romania, 2022, pp. 123–126.

[6] M. H. ZIKO, A. KOEL, T. RANG and J. TOOMPUU, *Analysis of barrier inhomogeneities of p-type Al/4H-SiC Schottky barrier diodes*, Materials Science Forum **1004**, 2020, pp. 960–972.

[7] P. M. GAMMON, A. PÉREZ-TOMÁS, V. A. SHAH, O. VAVASOUR, E. DONCHEV, J. S. PANG, M. MYRONOV, C. A. FISHER, M. R. JENNINGS, D. R. LEADLEY and P. A. MAWBY, *Modelling the inhomogeneous SiC Schottky interface*, Journal of Applied Physics **114**(22), 2013, paper 223704.

[8] R. T. TUNG, *Recent advances in Schottky barrier concepts*, Materials Science and Engineering: R: Reports **35**(1-3), 2001, pp. 1–138.

[9] G. PRISTAVU, G. BREZEANU, M. BADILA, R. PASCU, M. DANILA and P. GODIGNON, *A model to non-uniform Ni Schottky contact on SiC annealed at elevated temperatures*, Applied Physics Letters **106**(26), 2015, paper 261605.

[10] G. BREZEANU, G. PRISTAVU, F. DRAGHICI, R. PASCU, F. DELLA CORTE and S. RASCUNA, *Enhanced non-uniformity modeling of 4H-SiC Schottky diode characteristics over wide high temperature and forward bias ranges*, IEEE Journal of the Electron Devices Society **8**, 2020, pp. 1339–1344.

[11] R. PASCU, G. PRISTAVU, D.-T. ONEATA, M. STOIAN, C. ROMANITAN, M. KUSKO, F. DRAGHICI and G. BREZEANU, *Enhanced method of Schottky barrier diodes performance assessment*, Romanian Journal of Information Science and Technology **26**(2), 2023, pp. 181–192.

[12] G. BREZEANU, G. PRISTAVU, F. DRAGHICI, M. BADILA and R. PASCU, *Characterization technique for inhomogeneous 4H-SiC Schottky contacts: A practical model for high temperature behavior*, Journal of Applied Physics **122**(8), 2017, paper 084501.

[13] A. E. ARVANITOPOULOS, M. ANTONIOU, M. R. JENNINGS, S. PERKINS, K. N. GYFTAKIS, P. MAWBY and N. LOPHITIS, *A defects-based model on the barrier height behavior in 3C-SiC-on-Si Schottky barrier diodes*, IEEE Journal of Emerging and Selected Topics in Power Electronics **8**(1), 2020, pp. 54–65.

[14] G. PRISTAVU, D. T. ONEATA, R. PASCU, M. C. SERBANESCU, A. ENACHE, F. DRAGHICI and G. BREZEANU, *Modeling forward characteristics of high temperature capable Schottky diodes - High-accuracy optimization methods*, Proceedings of 2023 International Semiconductor Conference, Sinaia, Romania, 2023, pp. 85–88.

[15] H. DOĞAN, S. DUMAN, Y. TORUN, S. AKKOYUN, S. DOĞAN and U. ATICI, *Neural network estimations of annealed and non-annealed Schottky diode characteristics at wide temperatures range*, Materials Science in Semiconductor Processing **149**, 2022, paper 106854.

[16] A. RABEHI, B. NAIL, H. HELAL, A. DOUARA, A. ZIANE, M. AMRANI, B. AKKAL and Z. BENAMARA, *Optimal estimation of Schottky diode parameters using a novel optimization algorithm: Equilibrium optimizer*, Superlattices and Microstructures **146**, 2020, paper 106665.

[17] W. FILALI, R. AMRANI, E. GAROUDJA, S. OUSSALAH, F. LEKOUI, Z. OUKERIMI, N. SENGOUGA and M. HENINI, *Optimal identification of Be-doped Al0.29Ga0.71As Schottky diode parameters using Dragonfly Algorithm: A thermal effect study*, Superlattices and Microstructures **160**, 2021, paper 107085.

[18] H. DOĞAN, *Parameter estimation of AI/p-Si Schottky barrier diode using different meta-heuristic optimization techniques*, Symmetry **14**(11), 2022, paper 2389.

[19] Y. TORUN and H. DOĞAN, *Modeling of Schottky diode characteristic by machine learning techniques based on experimental data with wide temperature range*, Superlattices and Microstructures **160**, 2021, paper 107062.

[20] A. B. ÇOLAK, *An experimental study on the comparative analysis of the effect of the number of data on the error rates of artificial neural networks*, International Journal of Energy Research **45**(1), 2021, pp. 478–500.

[21] T. GÜZEL and A. B. ÇOLAK, *Investigation of the usability of machine learning algorithms in determining the specific electrical parameters of Schottky diodes*, Materials Today Communications **33**, 2022, paper 104175.

[22] K. ROBERTS, *A robust approximation to a Lambert-type function*, ArXiv:1504.01964, 2015, pp. 1–8.